Catalysis Today 166 (2011) 123–128

Contents lists available at ScienceDirect

Catalysis Today

journal homepage: www.elsevier.com/locate/cattod

Influence of nitrogen on the catalytic behaviour of Pt/γ-Al_2O_3 catalyst in glycerol reforming process

Nian-Jun Luo[a], Jin-An Wang[b], Tian-Cun Xiao[a,c], Fa-Hai Cao[a,*], Ding-Ye Fang[a]

[a] State-Key Laboratory of Chemical Engineering, ECUST, No. 130, Meilong Road, Shanghai 200237, China
[b] Laboratorio de Catálisis y Materiales, ESIQIE, Instituto Politecnico Nacional, Col. Zacatenco, C. P. 07738 México D.F., Mexico
[c] Inorganic Chemistry Laboratory, Oxford University, OX1 3QR Oxford, UK

ARTICLE INFO

Article history:
Available online 18 May 2010

Keywords:
Glycerol
Nitrogen
Deactivation
Coke

ABSTRACT

In the present work, deactivation behaviour of a Pt/γ-Al_2O_3 catalyst used for converting glycerin/water mixture into hydrogen was investigated. It was shown that main reason for the catalyst activity drop is due to the carbon deposition over the catalyst surface. Interestingly, the catalyst suffered from faster deactivation in the case of nitrogen presence in the inlet stream. However, the catalytic stability of the catalyst could be greatly enhanced when nitrogen was phase out from the reaction atmosphere. In the reaction mixture containing 10 wt% glycerol, the deactivation constant of the catalyst decreased from $d_A = -0.0516$ mL/(min $g_{cat.}$ h) under a condition with nitrogen to $d_B = -0.0051$ mL/(min $g_{cat.}$ h) without nitrogen in the reaction bed. Catalytic evaluation and thermogravimetric analysis revealed that nitrogen was not only an inert carrier gas served as but also an accelerator for coking. A speculation model was proposed for explanation of the coking process over the catalyst with the nitrogen effect.

1. Introduction

Renewable fuel production has been increasingly demanded due to growing concern over global warming and energy security. The exponential increase of biodiesel production [1] via *trans*-esterification produced glycerol as the side product, leading to surplus supply of glycerol with low value. Hence, new applications of this new derived side product are urgently needed to make use of them. Besides converting glycerol into value-added chemicals [2–5], hydrogen production from glycerol reforming [6–13] or pyrolysis [14] is an attractive alternative for renewable hydrogen generation. The desirable pathway is that glycerol undergoes decomposition to produce CO and H_2 (Eq. (1)), followed by water–gas-shift (WGS) reaction (Eq. (2)) to convert CO into CO_2 with additional hydrogen:

$$\text{glycerol decomposition}: \quad C_3H_8O_3 \rightarrow 3CO + 4H_2 \tag{1}$$

$$\text{WGS reaction}: \quad CO + H_2O \rightarrow CO_2 + H_2 \tag{2}$$

However, during the real reforming process, side reactions always occur [15,16] to produce liquid by-products and/or char, which would reduce hydrogen yield and/or impair activity and stability of the catalyst, as shown in Fig. 1.

Fig. 2 shows a molar triangular diagram of carbon–hydrogen–oxygen equilibrium phase for gasification or reforming system [17,18]. On the basis of this phase diagram, to avoid carbon formation, additional oxygen or hydrogen is needed to shift the equilibrium point to shaded section below the carbon decomposition boundary (dashed line), where carbon is present as CO, CO_2 and CH_4. Ideally, glycerol with C/O ratio of 1 does not require additional oxygen to break it down to CO and H_2.

Carbon easily formed during steam reforming process and consequently resulted in catalyst deactivation, but this formation could be thermodynamically inhibited under the conditions of temperature >627 °C, atmospheric pressure and a molar ratio of water/glycerol of 9:1 according to Adhikari's report [19]. Comparatively speaking, liquid reforming for hydrogen production could alleviate the catalyst deactivation and decrease the CO content under lower temperature [9,20,21]. However, in the actual reforming process, more carbon was still formed than predicted. Thus it is of high interest to study the coking behaviour.

In the present study, deactivation resulted from carbon formation during the liquid reforming process of converting glycerol into hydrogen was investigated. In our experiments, coke formation was found to be the main reason for the deactivation of platinum catalyst. The presence of nitrogen in the catalytic reaction bed could accelerate the coking rate, which would be alleviated by improving the technological route to phase nitrogen out of the reaction area. Usually, inert gas of nitrogen is used as carrier gas or standard criterion or due to other causes, while its effect on

* Corresponding author. Tel.: +86 21 64252874.
E-mail address: fhcao@ecust.edu.cn (F.-H. Cao).

0920-5861/$ – see front matter © 2010 Elsevier B.V. All rights reserved.
doi:10.1016/j.cattod.2010.04.013

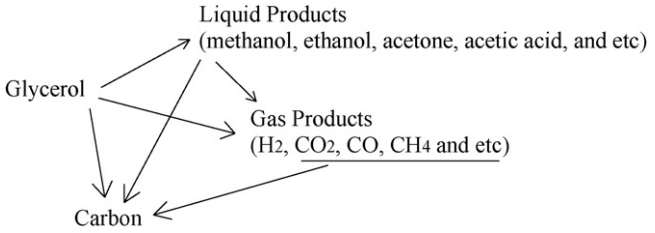

Fig. 1. Possible reaction pathways of glycerol reforming to hydrogen.

the reaction process was seldom studied [22,23]. Our studies show that nitrogen has significant influence on the catalysts deactivation; this new finding would facilitate avoiding quick deactivation of in-use catalyst from the standpoint of chemical engineering and technology.

2. Experimental

2.1. Catalyst preparation

Pt-based catalysts were prepared by means of incipient wetness method. Typically, γ-Al_2O_3 support (sieved to 178–250 μm) was impregnated with a desired amount of H_2PtCl_6 aqueous solution for 24 h at room temperature; it was then dried at 120 °C overnight in an oven and calcined at 260 °C for 2 h in air to produce the Pt/γ-Al_2O_3 catalyst.

2.2. Catalyst characterization

The specific surface area, pore volume and mean pore diameter were measured with an ASAP 2020 Micromeritics analyzer. The data were obtained from the nitrogen adsorption isotherm of the 500 °C calcined supports. The specific area was calculated from the Brunaur–Emmett–Teller (BET) equation and the mean pore size diameter from the Barrett–Joyner–Halenda (BJH) method. Before the measurements the samples were desorbed at 150 °C for 0.5 h.

The elemental analysis of the spent catalyst for carbon and hydrogen was carried out on the elemental analyser Vario EL. The sample was digested through oxidative combustion and the gases were analyzed with a thermal conductivity detector.

Powder X-ray diffraction (XRD) pattern of each sample was obtained with an X'Pert Pro Alpha 1 diffractometer using monochromic Cu Kα radiation (λ = 1.5406 Å; 40 kV, 30 mA). The specimen were prepared by grinding a small amount of each sample using an agate mortar and pestle and then loaded into a flat sample loader. The data were scanned from 25° to 80° (2θ) in steps of 0.05°, with time per step of 1.25 s.

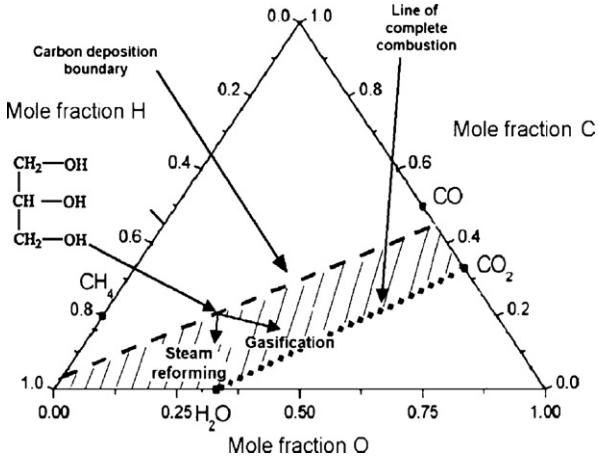

Fig. 2. Carbon–hydrogen–oxygen equilibrium phase [16].

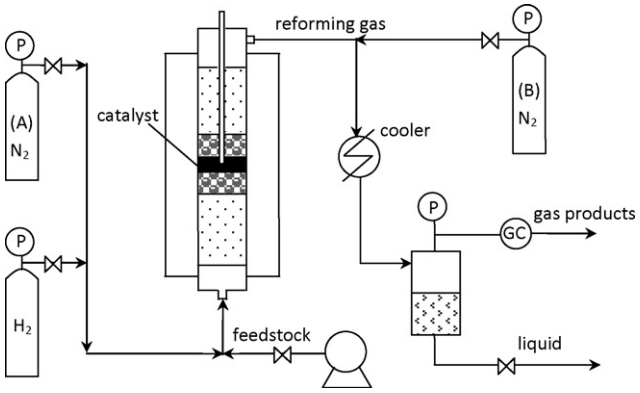

Fig. 3. Schematic setup of the evaluation apparatus for reforming glycerol/water mixture.

JEOL-JEM-1200EX transmission electron microscope (TEM) operating at 100 kV was employed to investigate the morphology of platinum particles dispersion on the catalyst.

The different platinum species was studied by laser Raman spectroscopy using a Yvon Jobin Labram spectrometer with a 632.8 nm HeNe, run in a back-scattered confocal arrangement. Raman spectra were recorded in air at room temperature with a resolution of 2 cm^{-1} and scanning range of 50–400 cm^{-1}.

Thermogravimetric (TG) analysis of the samples (100 mg) were conducted by Thermo-Thermax-700 using air (60 mL min^{-1}), heated from 25 °C to 800 °C at 10 °C/min. The gas effluents were followed by a quadrupole mass spectrometry.

2.3. Activity test

Liquid reforming of glycerol/water mixture (5 or 10 wt% glycerol) was performed in a stainless steel fixed tubular reactor of Ø 17 mm × 40 cm (see Fig. 3) where a catalyst sample (1 or 2 g) was loaded in the middle of the tube and quartz particles was filled in the two ends of the catalyst bed. Prior to a reforming test, the catalyst was reduced in flowing hydrogen (100 mL/min) at 260 °C for 2 h, and then nitrogen from cylinder-A was allowed to remove the remnant hydrogen and cool the system to room temperature. When a test began, the feedstock was pumped (0.05 or 0.10 mL/min) with a constant pump into the reactor. In the case of nitrogen presence in the catalytic bed, N_2 (30 mL/min from cylinder-A, with cylinder-B out of use) was co-fed into the reactor; and in the case of nitrogen absence in the catalytic bed, N_2 (30 mL/min from cylinder-B, with cylinder-A out of use) was pressurized into the cooler after the reactor to keep the system pressure constant (i.e. 25.0 bar at 220 °C) at a temperature. Nitrogen also took the roles of carrier gas and standard criteria for gas products' analysis. The reforming gas was analyzed with GC equipped with TCD detector connected in line with the chemical reactor. The amount of hydrogen produced was calculated as product of its percentage in outlet stream (gas) multiplied by the flow rate of outlet stream (gas), and then divided by gram of catalyst.

Hydrogen yield was calculated to be

$$\frac{\text{experimental hydrogen produced}}{\text{theoratical hydrogen produced}}$$

where

$$\text{theoretical hydrogen production} = \frac{F_{\text{solution}} \times \rho \times \text{wt\%}}{M_{\text{glycerol}}} \times 7 \times 22.4 \times 1000$$
$$= \frac{0.05\,\text{mL/min} \times 0.993\,\text{g/mL} \times 5\%}{92} \times 7 \times 22.4 \times 1000 = 4.231\,\text{mL/min}$$

under conditions of glycerol (5 wt%)/water mixture and feed rate of 0.05 mL/min.

3. Results and discussion

3.1. Presence of nitrogen in catalytic reaction bed

3.1.1. Activity test

With the presence of nitrogen in the catalytic bed, platinum catalysts with different loadings were investigated to perform liquid reforming of glycerol (5 wt%)/water mixture for hydrogen generation, and the results are shown in Fig. 4. It is seen that the highest amount of hydrogen nearly reached 2 mL/(min $g_{cat.}$) for 0.9 wt% Pt/γ-Al_2O_3. Both 1.2 wt% Pt/γ-Al_2O_3 and 0.6 wt% Pt/γ-Al_2O_3 catalysts behaved similar activity for hydrogen production, and 0.3 wt% Pt/γ-Al_2O_3 showed the lowest catalytic activity among them. However, all the catalyst activity dropped gradually with time-on-stream. To further understand the details about the deactivation, the fresh and spent catalysts were characterized by means of BET, XRD and elemental analysis of carbon and hydrogen.

3.1.2. Characterization results

3.1.2.1. Specific surface area determination. Table 1 displays the textural structure of both fresh and spent catalysts, as well as the results of carbon and hydrogen elemental analysis. As seen, the BET surface, pore volume and pore size were reduced after catalytic evaluation. The pore diameter of the spent catalyst was large enough (15 nm) to allow the reforming reaction occurring inside the inner channels because it was much greater than the size of glycerol molecule which is around 0.62 nm [24]. Thus, the deactivation may be not due to the diffusion limitation of the reactants or products. It is noted that surface area was reduced from 184.2 m^2/g for the fresh 0.9 wt% Pt/γ-Al_2O_3 catalyst to 145.5 m^2/g for the spent one, therefore, catalytic deactivation was probably related to reduction of surface area that might reduce the number of active sites. Additionally, the elemental analysis presented in weight ratio of carbon and hydrogen in/on catalyst was equal to 8.34 (7.18:0.86), which was much greater than that in glycerol molecule. This implied that carbon entities were formed on spent catalyst and they might occupy the active sites, for instance, covering the Pt site, consequently impaired the activity. Therefore, it can be regarded that the formation of carbon entities reduced the surface area and thus decreased the catalytic activity.

3.1.2.2. XRD. Fig. 5 shows the XRD patterns of both fresh and spent 0.9 wt% Pt/γ-Al_2O_3 catalysts. The spent catalyst exhibited new diffraction lines compared to the fresh one, representing formation of new phase in the catalyst. The new XRD peaks denoted as β were indentified to be boehmite $Al_2(OOH)_2$ that was generated from γ-Al_2O_3 hydration during the reaction condition. This result was in agreement with the TG results shown in the following section. The other unmarked new sharp lines were identified as SiO_2 that was introduced into the reactor to fix the catalyst in the middle and buffer the temperature change of feedstock.

3.1.2.3. TEM. The aggregation of active metal particles usually leads to catalytic deactivation. Our TEM images of both fresh and spent 0.9 wt% Pt catalyst (Fig. 6) indicates the fresh before reduction did not present Pt particles and the spent presented platinum particles with size of around 2–5 nm. No aggregation was observed and Pt atoms well dispersed on the catalyst support.

3.1.2.4. Raman. Around the above tests of four different platinum load catalysts, the highest load of 1.2 wt% Pt catalyst performed

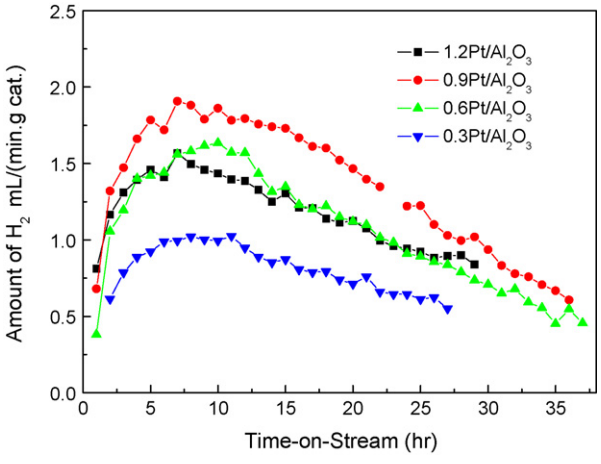

Fig. 4. Amounts of hydrogen produced in the presence of N_2 in catalytic area.

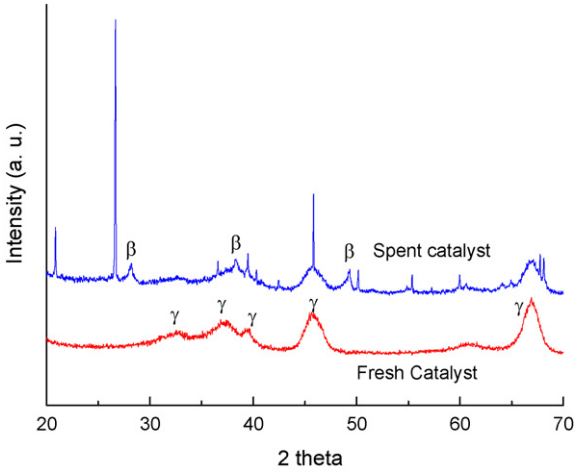

Fig. 5. XRD patterns of both fresh and spent 0.9 wt% Pt/γ-Al_2O_3.

Table 1
Data of catalyst structure analysis and elemental analysis.

Catalyst	Structure of catalysts			C, H elemental analysis	
	Surface area (m^2/g)	Pore volume (cm^3/g)	Pore size (nm)	C content	H content
Fresh 0.9 wt% Pt/γ-Al_2O_3	185.23	0.75	16.10	–	–
Spent 0.9 wt% Pt/γ-Al_2O_3	145.51	0.55	15.13	7.18 wt%	0.86 wt%

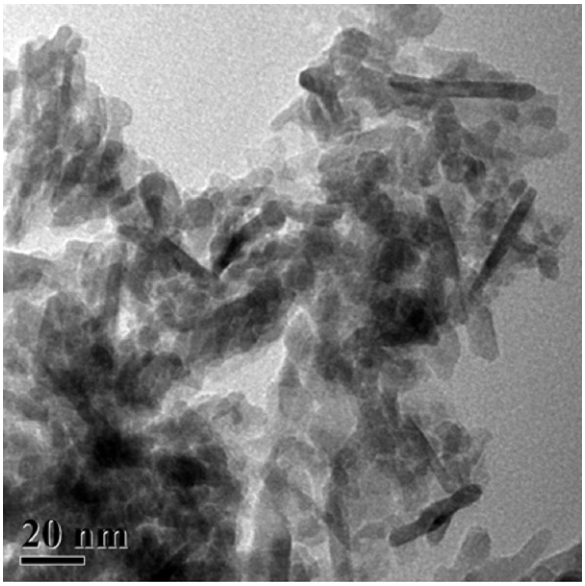

(a) TEM image of fresh 0.9wt%Pt/γ-Al_2O_3

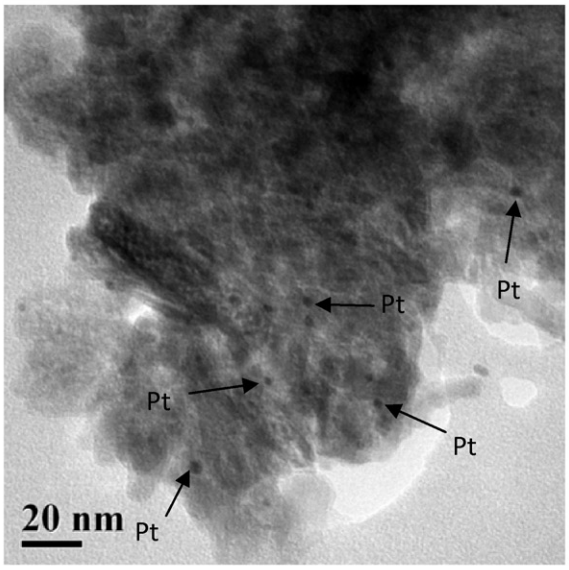

(b) TEM image of spent 0.9wt%Pt/γ-Al_2O_3

Fig. 6. TEM images of both fresh and spent 0.9 wt% Pt/γ-Al_2O_3.

lower activity than 0.9 wt% Pt catalyst. To probe the details, an initial Raman characterization was conducted with results shown in Fig. 7. In this figure, the peaks between 100–250 cm^{-1} resulted from Pt–Cl bond, which may attributed to species of $PtCl_6^{2-}$ or $PtCl_4^{2-}$ species. Chloride content was usually regarded to be detrimental to catalytic activity in reaction process [25]. Here 0.9 wt% Pt catalyst exhibited lower Cl^- content than 1.2 wt% Pt catalyst and thus produced higher hydrogen yield. The loss of Cl^- occurred during the calcinations process. To make sure this viewpoint based on Raman results, more details is under probing.

3.2. Absence of nitrogen in catalytic reaction bed

3.2.1. Activity test

The stability evaluation of the catalyst was also carried out with absence of nitrogen in reaction atmosphere. The 0.6 wt% Pt/γ-Al_2O_3 catalyst behaved much stable in comparison with the case of nitrogen presence in the catalytic bed, as illustrated in Fig. 8. The amount of produced hydrogen fluctuated around 2.5 mL/(min $g_{cat.}$) in the initial stage and then slowly decreased to 2.0 mL/(min $g_{cat.}$) up to 150 h. Of similar stabilization were both the produced carbon dioxide and methane, which was 1.0–1.2 mL/(min $g_{cat.}$) and less than 0.25 mL/(min $g_{cat.}$), respectively. In addition, the ratio of hydrogen to carbon dioxide was fluctuating between 2.0 and 2.2 during the reaction, close to the stoichiometric ratio of 2.33. These results showed that the catalytic stability of the platinum catalyst was improved with the absence oh nitrogen in the reaction system. In another word, the catalyst deactivation rate was relatively low in the condition of nitrogen absence in the reaction bed.

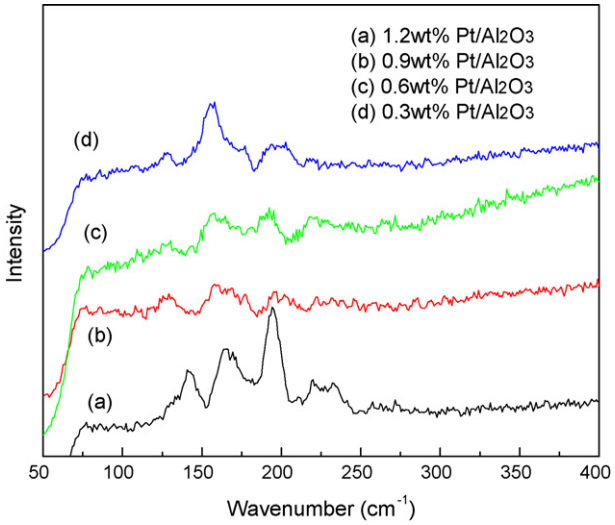

Fig. 7. Raman spectra of catalysts employed in reforming process.

3.2.2. Repeatability of test

Fig. 9 presents the influence of operation conditions on hydrogen yield and results of repeatability test under 220 °C & 25.0 bar and 240 °C & 35.0 bar. It is obvious that higher reaction temperature coupled with higher pressure would improve hydrogen yield of around 30% 200 °C & 16.4 bar up to about 75% under 240 °C & 35.0 bar, and the initial test has a similar results with the repeatable test, hence we regard the experimental data are of acceptance.

3.2.3. Kinetic analysis

The reforming results over 0.6 wt% Pt/γ-Al_2O_3 catalyst obtained in both cases of nitrogen absence and presence are comparatively

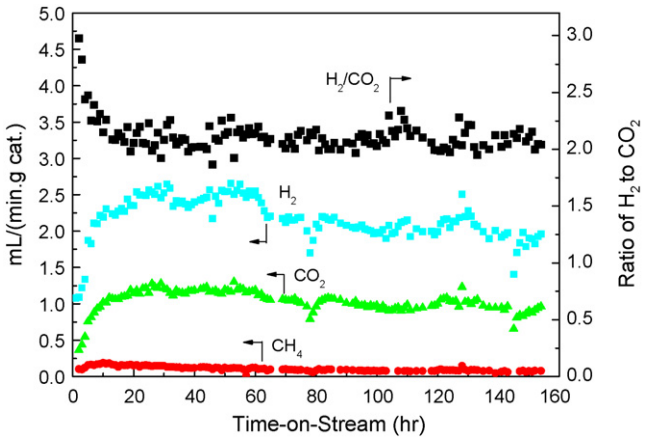

Fig. 8. Amounts of gas products produced with absence of nitrogen.

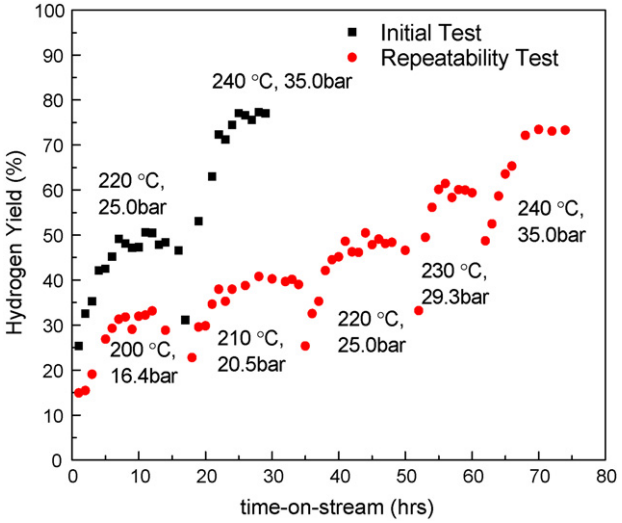

Fig. 9. The effect of reaction conditions and repeatability test.

shown in Fig. 10. It can be seen that nitrogen presence, whatever the glycerol concentration of 10 or 5 wt% was, would result in quick deactivation of catalyst with a similar pattern (Fig. 10A and C); whereas, without N_2 in the inlet stream, the catalytic stability of catalyst was greatly enhanced (Fig. 10B). The amount of hydrogen was cut off about 22% after 22 h of reaction (Fig. 10A) and around 75% after 38 h of reaction (Fig. 10C) for the reaction mixture with N_2. However, as shown in Fig. 10 B, the hydrogen amount was remained almost the same after 60 h of reaction, and it was just reduced by approximately 33% after 152 h of time-on-stream.

To clearly elucidate the difference of deactivation rate in both conditions of N_2 absence and presence in the catalytic area, simple deactivation equations (Eq. (3)) were linearly fit according to the data plot in Fig. 10 (from the peaks down):

$$\begin{pmatrix} R_A \\ R_B \\ R_C \end{pmatrix} = \begin{pmatrix} I_A \\ I_B \\ I_C \end{pmatrix} + \begin{pmatrix} d_A \\ d_B \\ d_C \end{pmatrix} t = \begin{pmatrix} 4.1675 \\ 2.6337 \\ 1.9789 \end{pmatrix} + \begin{pmatrix} -0.0516 \\ -0.0051 \\ -0.0423 \end{pmatrix} t \quad (3)$$

where R – amount of hydrogen produced, mL/(min $g_{cat.}$); t – time-on-stream, h; I – pseudo-initial amount of hydrogen produced at time-on-stream of 0 h; d – constant of catalyst deactivation, mL/(min $g_{cat.}$ h); A, B, C – the operation conditions shown in the notes of Fig. 10.

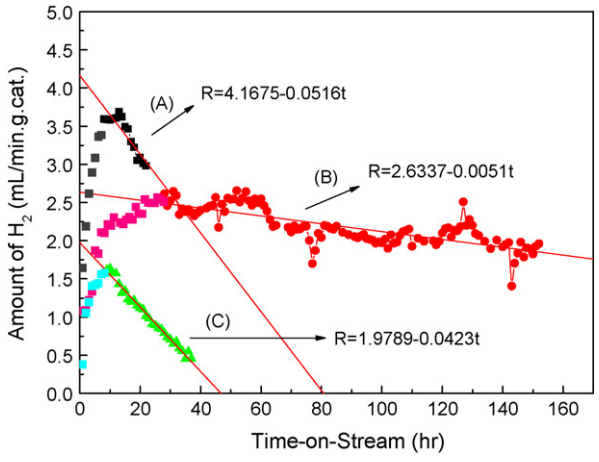

Fig. 10. Comparative results of catalyst deactivation with presence/absence of nitrogen.

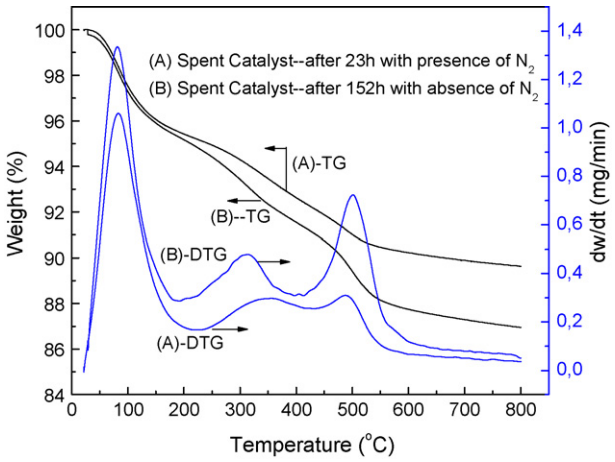

Fig. 11. TG curves and DTG curves for spent catalysts.

From this deactivation equation matrix, three different operation conditions produced different pseudo-initial hydrogen amount, and all the catalysts were deactivated to some extent. I_A was around twice of I_C due to the higher concentration of 10 wt% in operation (A) over 5 wt% in operation (C). However, I_A was also higher than I_B under the same concentration of glycerol and space velocity, which can be explained by the bulk diffusivity of gas products in nitrogen atmosphere [26]. In the presence of nitrogen in reaction area (A), the gas products can be easily extracted from the catalyst and soluble in nitrogen atmosphere, thus a higher hydrogen amount was obtained. While without nitrogen (B), the catalyst was involved in a water-dominated environment, and the gas products could not be easily removed from the catalyst and soluble into water, thus suppressed reaction to some extent from a viewpoint of reaction equilibrium and that resulted in a lower hydrogen amount. In addition, despite I_A was the highest among three of them, d_A of −0.0516 mL/(min $g_{cat.}$ h) also reflected the catalyst used in (A) suffered from most serious deactivation. As for the condition (B) without nitrogen, the catalyst lost its activity very slowly with d_B of −0.0051 mL/(min $g_{cat.}$ h), just around one tenth of d_A, which implied that catalyst could be stabilized under such operation condition. The catalyst employed in condition (C) also deactivated quickly due to presence of nitrogen, but d_C (−0.0423 mL/(min $g_{cat.}$ h)) was still slightly lower than d_A, and it may be related to the concentration of glycerol.

3.3. Carbon formation and coking

3.3.1. Thermogravimetric analysis

In order to investigate the influence of nitrogen on the catalyst deactivation, thermogravimetric analyses of the spent catalysts were carried out and the results are shown in Fig. 11.

Both TG curves exhibited three weight loss stages between 25 and 800 °C. The catalyst (B) after 152 h of reaction under the reaction condition without nitrogen in catalytic area produced a total 16 wt% weight loss and the other catalyst (A) after 23 h of reaction in the presence of nitrogen showed a total 10.5 wt% weight loss.

Three DTG peaks corresponded to (i) removal of physical absorbed water in/on catalysts (50–150 °C), (ii) conversion of new-formed boehmite during the reaction to γ-Al_2O_3 (250–350 °C) (Eq. (4)) [27]:

$$\gamma\text{-}Al_2(OOH)_2 \xrightarrow{\Delta} \gamma\text{-}Al_2O_3 + H_2O \quad (4)$$

and (iii) removal of coke by oxidation in air (450–550 °C).

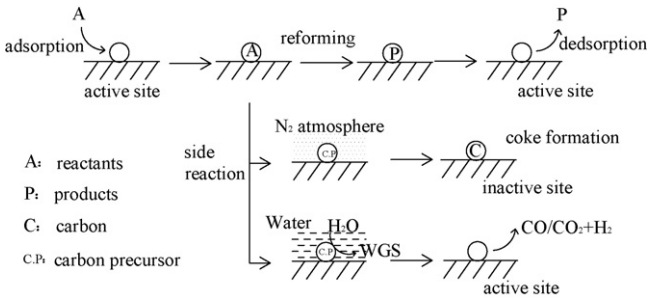

Fig. 12. Speculation model for coking behaviour in glycerol reforming process.

The mean coking rate on the spent catalyst in the absence of N_2 was calculated to be 0.0596 mg/($g_{cat.}$ h), lower than that of 0.1102 mg/($g_{cat.}$ h) in the case of N_2 presence during the reaction. It is also noted that the amount of boehmite was low when nitrogen was present in the inlet stream. Therefore, it can be concluded that it was coke formation rather than phase conversion of γ-Al_2O_3 into boehmite that dominated deactivation rate.

3.3.2. Coking model

The effect of inert gas carrier on the catalyst behaviour was seldom reported [22,23]. The experimental results presented in this work showed that nitrogen would, indeed, influence the catalytic activity and stability of the catalyst. The speculation model of coke formation on/in catalyst is presented in Fig. 12.

During the reaction, the reactants were adsorbed on an active site on which reforming reaction occurred to produce products, followed by desorption to release products and active site. However, side reaction accompanying with the desired reforming process took place to produce carbon precursors, such as absorbed CO, that would transform into coke ($2CO \rightarrow C + CO_2$) to occupy the active site, leading to the catalyst deactivation. In our experiments, when the reaction environment was nitrogen-dominated, the formed coke was not easily removed [28], hence, more coke deposits covered on the catalysts surface; whereas, as water stream dominating the catalytic bed, the carbon precursors likely reacted with water to produce CO/CO_2 and additional hydrogen via WGS reaction, and consequently, the rate of carbon formation was inhibited and the active site could be released rapidly, therefore, the catalyst stability was greatly enhanced. This postulated mechanism may be helpful in the understanding of the better stability of the catalyst used in a process without nitrogen in the catalytic reaction area.

4. Conclusions

This present work focused on the effect of nitrogen in the catalytic conversion of glycerol/water mixture into hydrogen. With nitrogen in the reaction stream, the catalyst displayed higher initial activity but poor stability, while in the case of nitrogen absence, better catalytic stability was achieved. Nitrogen absence in catalytic bed could alleviate deactivation rate to a large extent, despite it led to low hydrogen amount in the initial stage of reaction. Repeatability of test indicated that the experimental data were of acceptance and higher reaction temperature coupled with higher pressure would improve hydrogen yield.

The characterization results illustrated that carbon formation was mainly responsible for the deactivation and no aggregation of platinum particles occurred after use; chlorine might be detrimental to the catalytic activity. The presence of nitrogen in the reaction stream accelerated the carbon formation rate, thus leading to a faster activity drop. A coke formation mechanism in nitrogen atmosphere was proposed to elucidate the process of catalyst deactivation.

Acknowledgements

We are grateful to National High-Tech Research and Development Program of China (863 Program: 2009AA05Z444) and Foundation of Dalian Institute of Chemical Physics (N-08-05) for financial support.

References

[1] BIODIESEL 2020, A Global Market Survey, Feedstock Trends and Forecasts, 2nd ed., Emerging Markets Online, 2008.
[2] J.N. Chheda, G.W. Huber, J.A. Dumesic, Angew. Chem. Int. Ed. 46 (2007) 7164–7183.
[3] M. Balaraju, V. Rekha, P.S.S. Prasad, R.B.N. Pradad, N. Lingaiah, Catal. Lett. 126 (2008) 119–124.
[4] C. Zhou, J.N. Beltramini, Y. Fan, G. Lu, Chem. Soc. Rev. 37 (2008) 527–549.
[5] J. Feng, H.Y. Fu, J.B. Wang, R.X. Li, H. Chen, X. Li, Catal. Commun. 9 (2008) 1458–1464.
[6] P. Ramírez de la Piscina, N. Homs, Chem. Soc. Rev. 37 (2008) 2459–2467.
[7] A.J. Byrd, K.K. Pant, R.B. Gupta, Fuel 87 (2008) 2956–2960.
[8] E.L. Kunkes, R.R. Soares, D.A. Simonetti, J.A. Dumesic, Appl. Catal. B: Environ. 90 (2009) 693–698.
[9] G.D. Wen, Y.P. Xu, H.J. Ma, Z.S. Xu, Z. Tian, Int. J. Hydrogen Energ. 33 (2008) 6657–6666.
[10] Y. Cui, V. Galvita, L. Rihko-Struckmann, H. Lorenz, K. Sundmacher, Appl. Catal. B: Environ. 90 (2009) 29–37.
[11] A. Iriondo, V.L. Barrio, J.F. Cambra, P.L. Arias, M.B. Gueemez, R.M. Navarro, M.C. Sanchez-Sanchez, J.L.G. Fierro, Top. Catal. 49 (2008) 46–58.
[12] P.D. Vaidya, A.E. Rodrigues, Chem. Eng. Technol. 32 (2009) 1463–1469.
[13] M.L. Dieuzeide, Norma Amadeo. Chem. Eng. Technol. 33 (2010) 89–96.
[14] B.L. Dou, V. Dupont, P.T. Williams, H.S. Chen, Y.L. Ding, Bioresour. Technol. 100 (2009) 2613–2620.
[15] T. Valliyappan, N.N. Bakhshi, A.K. Dalai, Bioresour. Technol. 99 (2008) 4476–4483.
[16] N.J. Luo, X.W. Fu, F.H. Cao, T.C. Xiao, P.P. Edwards, Fuel 87 (2008) 3483–3489.
[17] M.J. Prins, K.J. Ptasinski, F.J.J.G. Janssen, Chem. Eng. Sci. 58 (2003) 1003–1011.
[18] M. Slinn, K. Kendall, C. Mallon, J. Andrews, Bioresour. Technol. 99 (2008) 5851–5858.
[19] S. Adhikaria, S. Fernando, S.R. Gwaltney, S.D.F. To, R.M. Brickac, P.H. Steeled, A. Haryantoa, Int. J. Hydrogen Energ. 32 (2007) 2875–2880.
[20] I.O. Cruz, N.F.P. Ribeiro, D.A.G. Aranda, M.M.V.M. Souza, Catal. Commun. 9 (2008) 2606–2611.
[21] R.R. Davda, J.A. Dumesic, Chem. Commun. 1 (2004) 36–37.
[22] W.H. Chen, A. Pradhan, S.J. Jong, T.Y. Lee, I. Wang, T.C. Tsai, S.B. Liu, J. Catal. 163 (1996) 436–446.
[23] F. Aberuagba, A.A. Susu, Chem. Eng. Process. 38 (1999) 179–196.
[24] K. Mees, Arch. Otorhinolaryngol. 239 (1984) 49–59.
[25] M. Paulis, H. Peyrard, M. Montes, J. Catal. 199 (2001) 30–40.
[26] X.W. Huang, C.B. Roberts, Fuel Process. Technol. 83 (2003) 81–99.
[27] W. Deng, P. Bodart, M. Pruski, B.H. Shanks, Micropor. Mesopor. Mater. 52 (2002) 169–177.
[28] F. Alenazey, C.G. Cooper, C.B. Dave, S.S.E.H. Elnashaie, A.A. Susu, A.A. Adesina, Catal. Commun. 10 (2009) 406–411.